

NOAA Technical Memorandum OAR ARL-238

MDIFF TRANSPORT AND DIFFUSION MODELS

Jerrold F. Sagendorf

Roger G. Carter

Kirk L. Clawson

Field Research Division

Idaho Falls, Idaho

Air Resources Laboratory
Silver Spring, Maryland
February 2001



**UNITED STATES
DEPARTMENT OF COMMERCE**

**Donald L Evans
Secretary**

**NATIONAL OCEANIC AND
ATMOSPHERIC ADMINISTRATION**

Scott B. Gudes
Acting Under Secretary for Oceans
and Atmosphere/Administrator

Oceanic and Atmospheric
Research Laboratories

David L. Evans
Director

Notice

This document was prepared as an account of work sponsored by an agency of the United States Government. The views and opinions of the authors expressed herein do not necessarily state or reflect those of the United States Government. Neither the United States Government, nor any of their employees, makes any warranty, express or implied, or assumes any legal liability or responsibility for the accuracy, completeness, or usefulness of any information, product, or process disclosed, or represents that its use would not infringe privately owned rights. Mention of a commercial company or product does not constitute an endorsement by NOAA/OAR. Use of information from this publication concerning proprietary products or the tests of such products for publicity or advertising is not authorized.

Table of Contents

	<u>Page</u>
Notice	ii
Abstract	vi
Introduction	1
Puff Transport	5
Diffusion Theory	7
Horizontal Diffusion	7
Vertical Diffusion	8
Stability Class Determination	9
Plume Impact Calculations	11
Theory	11
Grid Setup	11
Sampling Puffs at the Grid Points	12
Dropping Puffs	12
Displaying MDIFF Results	13
Radiological Dose Conversion	15
MDIFF Evaluation	17
Time History Comparisons	18
Future Improvements	23
References	25

List of Figures

	<u>Page</u>
Figure 1. INEEL mesonet stations located in southeastern Idaho indicating their placement relative to the INEEL, major cities and localities, and nearby mountains	1
Figure 2. A simple puff-trajectory model example illustrating the trajectory and growth of three sequential puffs released in a westerly wind (a-c), and then three more sequential puffs released into a southerly wind (d-f)	3
Figure 3. A simple Gaussian plume model example illustrating plume growth in a westerly wind (a) and in a southerly wind (b)	4
Figure 4. MDIFF TIC selection menu invoked from INEELViz	13
Figure 5. MDIFF RSAC selection menu invoked from INEELViz	14
Figure 6. Location of the tracer release stack and tracer sampling arcs	17
Figure 7. Example model concentration isopleth and SF ₆ analyzer concentration from Test 5 at 14:45 MDT. The two numbers in the plume represent the measured SF ₆ concentration at the location of the measuring equipment	19
Figure 8. Time history graph of modeled and measured average 5-minute SF ₆ concentrations at receptor site B8 during Test 5	19

List of Tables

	<u>Page</u>
Table 1. Power law exponent (p) values as a function of stability class	6
Table 2. Desert diffusion coefficients for use in Eqns. 5, 6 and 7	9
Table 3. Atmospheric tracer test summary	18
Table 4. Comparisons of daytime modeled/measured SF ₆ concentration ratios	20
Table 5. Comparisons of nighttime modeled/measured SF ₆ concentration ratios	21

Abstract

The Field Research Division of the National Oceanic and Atmospheric Administration's (NOAA) Air Resources Laboratory (ARLFRD) maintains a network of 33 meteorological stations (mesonet) in the Upper Snake River Plain of the State of Idaho. These stations provide a comprehensive record of meteorology for the U.S. Department of Energy's (DOE) Idaho National Engineering and Environmental Laboratory (INEEL) and surrounding area. One important use of the mesonet data is to drive transport and diffusion models that can be used for estimating impacts for both near real-time emergency response and for normal facility operations over long periods of time. This paper describes the MDIFF and MDIFFH models that have been developed to support those needs. The models are based on calculating transport of plume material using winds derived from the mesonet. Meteorological data from the mesonet are updated at five minute intervals. MDIFF uses the mesonet five-minute data to update trajectories also at five minute intervals. MDIFF is able to access the mesonet data in near real-time and is well suited for use in emergency operations. MDIFFH is designed for estimating impacts over periods of up to a year or more. It is driven by hourly data derived from the mesonet. A small field research project was conducted in 1999 where MDIFF was used to make real-time predictions of the location and concentration of an intentionally released atmospheric tracer gas plume. Results from this project are included in this paper as an evaluation of MDIFF.

Introduction

MDIFF and MDIFFH are computer models for estimating concentration patterns of airborne materials released from a single location. They were designed to use wind field data derived from the National Oceanic and Atmospheric Administration's (NOAA) Air Resources Laboratory Field Research Division's (ARLFRD) network of meteorological towers (mesonet) existing in the Upper Snake River Plain in the State of Idaho (Fig. 1). They are well suited for calculating the transport and dispersion of airborne material on and near the U.S. Department of Energy's (DOE) Idaho National Engineering and Environmental Laboratory (INEEL).

The models are based on the MESODIF computer program (Start and Wendell 1974). MESODIF (short for MESOscale DIFfusion) was one of the first puff diffusion models developed for use on modern computers. MDIFF and MDIFFH use the same basic algorithm to calculate atmospheric transport. The algorithm is conceptually very simple: 1) every release of material is represented as a series of puffs; 2) each puff is allowed to move and grow independently; 3) concentrations are calculated as the sum of the concentrations due to all of the puffs.

MDIFF is used to model short-term episodes. It can be initiated from ARLFRD's mesonet data visualization tool

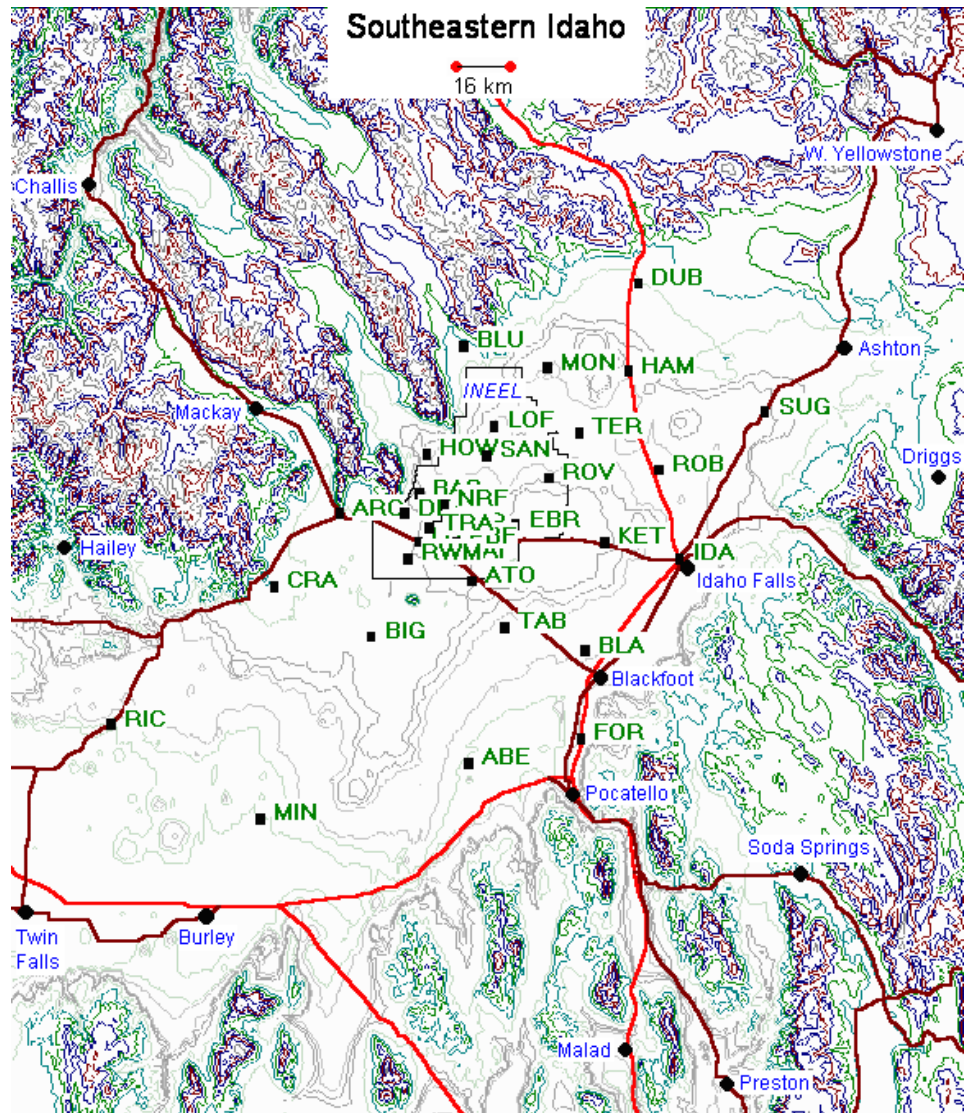


Figure 1. INEEL mesonet stations located in southeastern Idaho indicating their placement relative to the INEEL, major cities and localities, and nearby mountainous terrain.

known as INEELViz. It operates using the five-minute mesonet database. MDIFF divides each release into five-minute puffs with each puff containing the material released during a five-minute period. For example, if 60 kg of material were released in one hour at a constant rate, MDIFF would represent the release as 12 puffs, each containing 5 kg of material. The puffs are advected in five-minute time steps to match the five-minute mesonet database wind fields.

MDIFFH is used for annual or other long-term simulations. It is driven by wind fields from the one-hour Mesonet database. The user selects the puff increment (number of puffs released per hour) and the advection step size. The model interpolates between hourly wind fields to accommodate the selected advection step size.

MDIFF and MDIFFH remember the location of the center and the size of each puff. The puffs move independently based on the wind speed and direction at the location of their centers. The puffs also increase in size with the passage of time. Puff location and size are calculated at each advection interval or step. A puff's location after the next advection step is its current location plus the wind speed vector multiplied by the advection step size. Likewise, its new size will be the current size plus the growth rate multiplied by the advection step size. (The details of these calculations are discussed in sections 2 and 3.) To calculate a concentration at a given point, MDIFF merely sums the concentrations of all the puffs that overlap that point.

The most important idea in this method is that each puff moves independently. If the wind changes with time, the puffs' movements will reflect the change. If a puff moves to an area where the wind is different (e.g. near the mountains), its path will reflect the winds of that area. This is especially important on the INEEL where the winds can vary greatly because of nearby mountainous terrain. A simple example will illustrate how this works. Assume material is released for 30 minutes. For the first 15 minutes, the wind blows from west to east at 10 m s^{-1} . For the last 15 minutes, it blows from south to north at 10 m s^{-1} . The puff locations calculated by MDIFF are shown in Figs. 2a to 2f. At five minutes after the release starts (Fig. 2a) there is one puff located 3000 m east of the release site. (Note: 5 minutes or 300 seconds $\times 10 \text{ m s}^{-1} = 3000 \text{ m}$) At 10 minutes after the beginning of the release (Fig. 2b), the first puff is 6000 m east and a second puff is located at 3000 m east of the release site. Note that the first puff has grown larger as it moves. After 15 minutes (Fig. 2c), there are three puffs that have moved and grown in size as previously described. Then assume that the wind direction changes to blow from the south. The existing three puffs start moving north as do the new puffs being released (Figs. 2d, 2e, and 2f). After 30 minutes, the observer in the northeast part of the figure is exposed to concentrations from puffs 1 and 2.

This example also illustrates why this technique is preferred over a straight line Gaussian calculation that is used in many diffusion models. The straight line Gaussian assumes a steady state or unchanging wind. It then calculates concentrations at points downwind using a formula based on a Gaussian or normal distribution of material. If we were to apply this type of calculation in our example and use the initial wind speed and direction (westerly), the result would be a concentration profile similar to that shown in Fig. 3a. If we used the wind speed and direction from the second half of the time period (southerly), the result would be similar to that shown in Fig. 3b. This calculation does not account for the material that has blown east of the release site and now is being blown north. Neither of the straight line Gaussian plume

calculations show any concentration at the observer's location in the northeast corner. The conclusion we draw from this example is that puff model is a better choice for the INEEL than the simple straight line Gaussian plume algorithm.

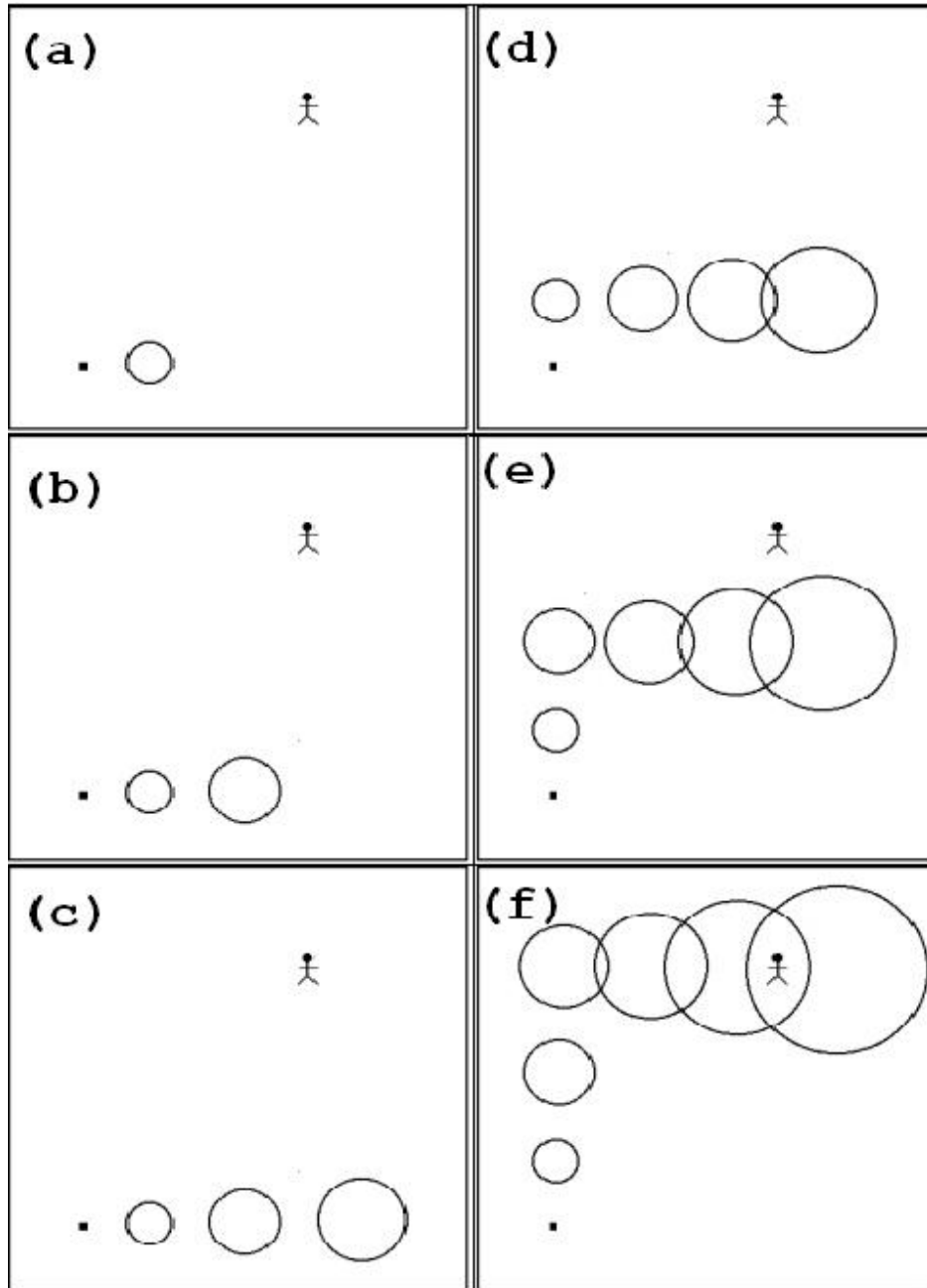


Figure 2. A simple puff-trajectory model example illustrating the trajectory and growth of three sequential puffs released in a westerly wind (a-c), and then three more sequential puffs released into a southerly wind (d-f).

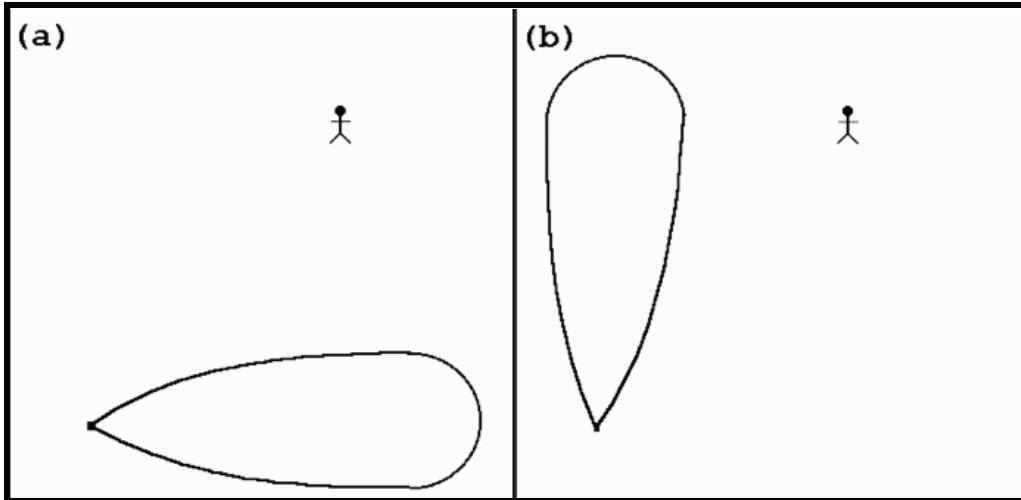


Figure 3. A simple Gaussian plume model example illustrating plume growth in a westerly wind (a) and in a southerly wind (b).

Puff Transport

Transport refers to the movement of plume material due to the movement of air (wind). MDIFF and MDIFFH account for transport by allowing the puffs to move with the wind. They simply calculate a new location for each puff at the end of each advection step interval. The calculation is very simple:

$$L' = L + (W_p \cdot \Delta t) \quad (1)$$

where L' is the new puff center location vector, L is the puff center location vector at the previous advection step, W_p is the average wind vector at the puff center during the advection step period, and Δt is the advection time step interval.

It is important to remember that this calculation is done only at the center of the puff. The models move the center of the puff and assume that the rest of the puff moves along with it. This is a good assumption as long as the winds do not vary greatly across the puff. When the puffs are small, this condition is generally valid. When the puffs become larger, it is not always true. One method of accounting for this is to split the puffs into several smaller puffs once they become large enough for this to be a problem. Experimentation with this technique in MDIFF has shown that there is little effect on the calculated concentrations. This is probably due to the fact that puffs that are large enough to be split, are so diffuse that they contribute very little to the total concentration. Consequently, the error caused by not splitting the large puffs tends to be quite small.

The more complicated part of this step is the calculation of W_p to be used. The required W_p must be determined at the location of the puff center and at the puff height. The first step in this process is correcting the winds for height. The winds used by MDIFF and MDIFFH are measurements made by the INEEL mesonet. Thirty towers in the mesonet have wind sensors placed 15 m above the ground. Three others have wind sensors placed at 10 m with a second set of wind sensors placed at a higher altitude between 46 and 76 m AGL. The winds obtained from all of these sensors must be corrected to the puff height before they are used. Typically, the puff height is specified when MDIFF is started. Optionally, MDIFF will calculate it using the Brigg's plume rise equations if requested to do so. (The Brigg's equations are not discussed here. See Briggs (1969) for a complete discussion.) Once the puff height is established, the tower wind speeds are corrected to this height with the following equation:

$$W_a = W \left(\frac{Z_a}{Z} \right)^p \quad (2)$$

where W_a the adjusted wind vector at height Z_a , W is the wind vector measured at height Z , Z_a is the puff height, Z is the height of the wind measurements, and p is the power law exponent. The exponent p is selected based on the current stability class, as given in Table 1. These exponents were derived from data obtained using the INEEL mesonet. The exponent p increases with increasing atmospheric stability, which produces higher wind speed aloft under stable atmospheric conditions than under stable atmospheric conditions.

Table 1. Power law exponent (p) values as a function of stability class.

Stability Class	p
A	0.093
B	0.106
C	0.112
D	0.182
E	0.287
F	0.331

Once the winds are corrected to the puff height, they are interpolated to the puff center location using a weighted average technique:

$$W_p = \frac{\sum W_{ai} (1/d_i)^2}{\sum (1/d_i)^2} \quad (3)$$

where W_p is the wind vector at the puff location, W_{ai} is the height-adjusted wind from tower i , and d_i is the distance from the puff center to tower i . By weighting the winds by the inverse square of the distance from the puff to the tower, nearby measurements are weighted much more heavily than distant measurements and the resultant average will closely follow nearby winds. This interpolated wind, W_p , may now be used directly to calculate a new puff location.

Diffusion Theory

The familiar Gaussian plume model has been in wide use for many years. It is attractive because it makes physical sense, it can be solved analytically, and it is well known and accepted by regulatory agencies. However, it assumes that plume material is released at a constant rate and, as previously noted, that the meteorological conditions remain steady, both in time and space, for a period of time longer than the dispersion time. The concept of a puff model is used to eliminate the “steady state” conditions that very often are not met in the real world. A series of puffs can be used to simulate the plume. Each puff is advected by a wind defined by the wind field at the puff location and at the current time step, and allowed to grow via Gaussian diffusion.

If we assume an instantaneous point source of material diffusing in three dimensions with total reflection at the earth's surface then the Gaussian instantaneous point-source (IPS) equation (Slade, 1968) can be written as follows,

$$\chi(\mathbf{x}, \mathbf{y}, \mathbf{z}, t) = \frac{Q(2\pi)^{-3/2}}{\sigma_x \sigma_y \sigma_z} \exp\left(-\left[\frac{(\mathbf{x} - \bar{u}t)^2}{2\sigma_x^2} + \frac{(\mathbf{y} - \bar{v}t)^2}{2\sigma_y^2} + \frac{(\mathbf{h} - \mathbf{z})^2}{2\sigma_z^2} + \frac{(\mathbf{h} + \mathbf{z})^2}{2\sigma_z^2}\right]\right) \quad (4)$$

where Q is the source strength, χ is concentration, x , y , & z are the coordinates in space, t is the time of travel from the point of release, h = effective plume height, \bar{u} is the average wind speed in the x direction, \bar{v} is the average wind speed in the y direction, and σ_x , σ_y , σ_z are the standard deviations of effluent in the downwind, crosswind, and vertical directions respectively.

Equation 4 is the starting point for deriving the familiar Gaussian plume equation. In that case, it is assumed that a continuous release takes place under steady state conditions. It is further assumed that diffusion in the direction of travel can be neglected in comparison with transport by the wind. In the case of a puff model, no steady state assumptions need be made. Puff travel and rate of growth are allowed to vary in space and time. In diffusion calculations, it is customary to assume that atmospheric conditions may be specified as stability classes ranging from very unstable to very stable. A very stable atmosphere tends to inhibit diffusion, whereas a very unstable atmosphere enhances diffusion. Puff growth is simply calculated as a function of atmospheric stability class and travel distance.

Horizontal Diffusion

It is assumed that diffusion in the along-wind and cross-wind directions is identical. In other words, σ_y is equal to σ_x and the puff grows as a spreading disk with a Gaussian distribution of material in the horizontal. To better conform to observed plume behavior, MDIFF considers two regimes for horizontal diffusion. For puffs that have traveled less than 20 km, the horizontal rate of growth is proportional to distance traveled raised to the 0.85 power. For puffs that have traveled more than 20 km, the horizontal growth rate is slowed to the Fickian rate (proportional to the square root of time or distance). The equations describing the growth of σ_y are represented by the general forms (Slade, 1968),

$$\sigma_y = \mathbf{A}_1 \times \mathbf{x}^{0.85} \quad (\mathbf{x} < \mathbf{20 km}) \quad (5)$$

and

$$\sigma_y = \mathbf{A}_2 \times \mathbf{x}^{0.5} \quad (\mathbf{x} > \mathbf{20 km}) \quad (6)$$

where x is the distance traveled by the puff, A_1 is the stability category-dependent coefficient for distances < 20 km, and A_2 is the stability category-dependent coefficient for distances > 20 km.

Vertical Diffusion

Vertical diffusion must account for constraints on vertical puff growth. The source is assumed to be at or near the surface of the earth, which acts as a physical barrier to downward puff growth. This is accounted for in Eq. 4 by the assumption of total reflection at the earth's surface. A capping stable layer also limits upward puff growth. The height of this layer is called the mixing depth. This layer divides the puff growth into three regimes. They are as follows.

1. A regime where the upward spread of the plume is not affected by the capping layer in which Gaussian diffusion is assumed.
2. A regime where the upward spread of the plume begins to be affected by the capping layer in which vertical distribution undergoes a transition between Gaussian and uniform.
3. A regime where the plume is thoroughly mixed in which the distribution of effluent is uniform between the ground and the capping lid.

The mixing depth is assumed to be constant in space but not in time. Currently, mixing depths are input from a file of climatological values as a function of the day of year and the time of day. It is hoped that in the future, real-time measurements of actual mixing depths will be available for use.

In MDIFF, the transition zone (second regime) begins when σ_z has reached 0.335 times the mixing depth. The uniform zone (third regime) begins when σ_z has reached 0.8 times the mixing depth. In the uniform zone, σ_z remains constant. The basic representation of σ_z is:

$$\sigma_z = \mathbf{B} \times \mathbf{x}^\gamma \quad (7)$$

where B is the stability-dependent coefficient, x is the distance traveled by the puff, and γ is the stability-dependent exponent of travel distance.

Table 2 contains the diffusion coefficients used in Eqns. 5, 6, and 7. These coefficients were formulated by Start and Wendell (1974) to fit a set of diffusion data collected at the National Reactor Testing Station, now known as the Idaho National Engineering & Environmental Laboratory, and the Hanford Site in the early 1960's (Markee, 1963, Fuquay et al., 1963). MDIFF also has the option to use the "Briggs open country" sigma curves (Briggs, 1973 and Gifford, 1976).

Table 2. Desert diffusion coefficients for use in Eqns. 5, 6 and 7.

Stability Class	A ₁	A ₂	B	γ
A	0.718	23.0	0.100	1.033
B	0.425	13.6	0.105	0.975
C	0.349	11.2	0.128	0.891
D	0.267	8.55	0.146	0.824
E	0.299	9.57	0.331	0.567
F	0.401	12.8	0.812	0.307

Since MDIFF allows the stability class to change during the course of an event, σ_z and σ_y cannot be calculated from equations 4, 5, and 6 as a simple function of travel distance and stability class. Start and Wendell (1974) calculated $\sigma = \sigma_0 + \Delta\sigma$, where σ_0 is the previous value and $\Delta\sigma$ is the incremental value calculated with the differentiated equations 5, 6, and 7. Another approach is the virtual distance method used by the puff model MESOI (Ramsdell, et al, 1983). Since this approach is computationally faster and gives the same results, it is used in MDIFF. The technique involves three steps:

1. At the beginning of each sampling interval, the current stability class and values of σ_y and σ_z are used to calculate distances to a virtual point source.
2. The travel distance during the sampling interval is then added to the virtual distance to get an effective travel distance.
3. Values of σ_y and σ_z are determined at the end of the sampling step from equations 5, 6, and 7 using the effective travel distance and current stability class.

Stability Class Determination

There are four options available for determining the atmospheric stability class. The first is from Markee (1963). It has the advantage of being defined for the INEEL area but it has the disadvantage of requiring an estimate of cloud cover. It also uses estimates of the solar angle by the season of the year, which creates discontinuities at the boundaries of the seasons. This method is also described in the Climatology of the Idaho National Engineering Laboratory (Clawson et al., 1989).

The second and third methods are described in the On-Site Meteorological Program Guidance manual of the Environmental Protection Agency (EPA, 1993). One method uses solar radiation in the daytime, temperature gradient at night, and wind speed. The other method uses the standard deviation of the horizontal wind direction and wind speed to determine stability class. These two methods have the advantage of being determined entirely by measured data, and they also enjoy the approval of the EPA. The disadvantage of each is that they tend to favor the neutral stability class at the expense of the stable and unstable classes. In southeastern Idaho,

neutral stability tends to be transitory, and is not observed as often as in areas that have moister climates. Hence, methods two and three may be more appropriately used in climates that are not as dry as that of Idaho.

The fourth method was developed at the Los Alamos National Laboratory for a desert climate somewhat similar to that of the INEEL (Bowen, Dewart, and Chen, 1983). The method is comparable to one of the EPA methods in that it uses solar radiation during the daytime, temperature gradient at night, and wind speed to designate stability class. It does not however, favor the neutral stability class to the same extent and may be more applicable to the INEEL. Using this method also has the advantage of determining the stability class by measured variables.

Plume Impact Calculations

Theory

Total integrated concentration (TIC) values are normally calculated by integrating the familiar Gaussian continuous point source equation with respect to x (the flow axis). This, however, is only applicable for straight-line flow. To calculate a TIC from a puff model, the contributions to the TIC from each puff must be summed as the puff passes the receptor. Using the finite difference equation we can approximate TIC values:

$$\text{TIC} = \sum_{j=1}^n (\chi_{\text{IPS}} \delta t)_j \quad (8)$$

where n represents the number of puffs. By using more puffs, the TIC integral may be approximated to any desired accuracy.

Grid Setup

A grid of receptors is established in each of the models for calculating concentrations. However, grid setup for the two models is handled differently. MDIFFH is generally used for long-term releases, which means large areas will be impacted. For this model, the total number of allowed grid points is defined at the time the program is compiled. The user selects the grid center and spacing at run time. Since the number of grid points is fixed, this means that selecting a fine-mesh grid decreases the area covered. As an example, for annual calculations where the main interest is the Upper Snake River Plain beyond the site boundaries, a 70 x 70 grid with 2 km spacing works nicely. If the area of concern were closer to the release point, then a finer-mesh grid with a smaller area of coverage would be more appropriate.

The MDIFF model is used for short-term releases such as might be encountered in emergency situations. The design of a receptor grid for a model such as MDIFF must balance grid point resolution and computational speed. Obviously, more grid points allow a finer-mesh on the grid, which leads to better results. This comes, however, at the expense of computational speed. MDIFF makes efficient use of grid points by running in two stages. The first stage of an MDIFF simulation calculates the puff trajectories. The program keeps track of the area of impact in this stage. In the second stage, the grid is built to fit a rectangular area encompassing the area of impact. MDIFF operates on a grid of up to 250,000 receptor positions in a 500 x 500 array. The distance between grid points is set in a configuration file. MDIFF will use that grid spacing, as long as there are enough grid points to cover the area of impact. If the area of impact is too large, MDIFF will adjust the grid spacing until the grid fills the needed area. There is also an option to allow MDIFF to determine its own grid spacing. In this case, grid point resolution is related to the area of coverage. The smaller the area needed to be covered, the finer the resolution will be.

Sampling Puffs at the Grid Points

Regardless of how fine the mesh, the operational grid consists of a finite number of grid points. The summing of concentrations at these grid points also must occur in a finite number of sampling steps. During an advection time step, it is possible for a puff to leapfrog over one or more grid points. This is especially true if wind speeds are high during the early stages of a simulation when the puffs are small. For these reasons, care must be taken to insure that the sampling of the puffs at the grid points is sufficient to obtain reasonable estimates of the plume impact. The MDIFF and MDIFFH models address this problem by assuring that each puff is sampled several times during each time step. The first step in the procedure is to compare the puff diameter to the grid spacing to determine if multiple grid points may be impacted by the puff. The desired step size is then determined by:

$$\text{StepSize} = \text{GridPts} \times \frac{3\sigma_y}{8} \quad (9)$$

where the puff diameter is assumed to be $3\sigma_y$, and GridPts is the number of grid points affected. MDIFF doesn't allow GridPts to be less than one. The above equation is designed to calculate a step size that will allow a puff to be sampled about 8 times. Note that if only one grid point is affected, the puff could be sampled 8 times as it passes over that grid point. If two grid points are affected, then the step size is such that the puff could be sampled 4 times at each grid point. The models then determine the number of steps needed within the advection step to achieve the desired sample step size using the following equation:

$$\text{NumSteps} = 1 + \frac{\text{TravelDist}}{\text{StepSize}} \quad (10)$$

where TravelDist is the distance the puff travels during the advection step. It should be noted that the above process insures only that puffs will be adequately sampled at grid points in their path. It doesn't guarantee, however, that the puffs will hit a grid point. Close to the source, it is possible for puffs smaller than the grid point spacing to slip between grid points. There will always be a region that is too close to the source for the model to properly resolve concentrations. As a general rule, a finer grid point mesh decreases the area near the source where this phenomenon might occur.

Dropping Puffs

MDIFF and MDIFFH track a puff until one of the following occurs:

1. The tracking time limit is met. The tracking time is the length of time the event will be simulated as specified by the user at run time. The user also specifies the length of the release, which translates to the number of puffs released. There is a limit of 24 hours for the release that is imposed by MDIFF. MDIFFH has no limit on the length of release. It is often used for continuous releases for a one-year period.
2. The program reaches the end of the mesonet data stream. For MDIFF, the data stream runs out at or near the current time of day unless the forecast mode is enabled. In that case, one or

two hours of forecast data is available, allowing MDIFF to make a short-term projection. Forecast data is provided outside of the MDIFF program by a pattern-matching scheme that searches for a similar wind field from historical data.

3. The puff leaves the area covered by the mesonet. The puff is assumed to be out of the area when it has traveled farther than 30 km from the nearest mesonet tower. When that distance is reached, the puff is considered to be outside of the mesonet domain. The puff is then simply dropped from consideration.

It should be noted that the INEEL mesonet covers a distance of over 160 km across the breadth of the Upper Snake River Plain. On simulations of a few hours duration, puffs seldom leave the area of mesonet coverage. Puffs may be tracked in the Snake River Plain from an area southwest of Aberdeen to an area northeast of Dubois.

Displaying MDIFF Results

MDIFF, the short-term model, may be initiated from within INELViz. At the completion of the simulation, a set of isopleths is transmitted to INELViz for display. The user may choose to display isopleths representing either a total integrated concentration (TIC) as in Fig. 4, or a radiological dose as in Fig. 5. The radiological dose is designed to be used in the INEEL Emergency Operation Center from pre-calculated scenarios. Usage of the radiological option is described in the next section.

The TIC option defaults to a release rate of 1 unit sec^{-1} where unit represents mass (grams, kg, curies, etc.). The resulting isopleths are then normalized by the source strength and one can simply multiply this value by the source strength to obtain a total integrated concentration. For example if we assume that the source unit is grams, the units on the isopleths would be $\text{g}\text{-sec m}^{-3}$. Note that this is a unit of dose and includes the exposure time. In the TIC option, the user may elect to select the isopleth values that are contoured, or the program will make it's own selection. The user may also enter up to 4 different release rates and the length of time they apply. In that case, the isopleth values reflect a true rather than a normalized TIC and include the amount of material released during the simulation. The user may also

The screenshot shows a software dialog box titled "Create Trajectory and Isopleth" with a "Release Settings" tab. The interface is divided into three main sections: "Release Location", "Release Description", and "Calculation Description".

- Release Location:** Includes a dropdown menu for "INTEC", radio buttons for "Site" (selected) and "Lat/Long", a "Begin Time" field set to "02/02/2001 1300", and "Height" set to "76.20 Meters".
- Release Description:** Features radio buttons for "Total Integrated Concentration" (selected) and "RSAC Dose Calculation". It contains two tables:

Rate (Units/sec)	Duration (HH:MM)
1.0	1:00
1.0	1:00
1.0	1:00
1.0	1:00
- Calculation Description:** Includes "Tracking Duration (HH:MM)" set to "1:00", "Contour Levels (0.00E-00)" set to "10 Contours", and a list of five "default" values for isopleth levels.

At the bottom of the dialog are three buttons: "Cancel", "Reset", and "Begin Process".

Figure 4. MDIFF TIC selection menu invoked from INELViz.

elect to run the model to display either a plume footprint or a plume snapshot from the Release Settings menu. The footprint represents the total accumulation for the entire tracking time, while the snapshot displays the average concentration over the last 5 minutes of the simulation.

Create Trajectory and Isoleth

Release Settings

Release Location

INTEC Site Begin Time 02/02/2001 1045
 43:33:59 N Lat/Long
 112:56:05 W Height 0.00 Meters

Release Description

Total Integrated Concentration
 RSAC Dose Calculation
 RSAC Dose File: 756FILTR Dose Pathways: Total Dose
 Duration (HH:MM): 1:00 % of Total Release: 100

Calculation Description

Tracking Duration (HH:MM): 1:00 Contour Levels (0.00E-00): 9 Contours

default	
default	
default	

Cancel Reset Begin Process

Figure 5. MDIFF RSAC selection menu invoked from INEELViz.

Radiological Dose Conversion

MDIFF is designed to estimate average and total integrated concentrations (TIC) of airborne materials. However, for emergency response operations at the INEEL, a primary concern is the release of radioactive materials. If radioactive materials are released, emergency responders may prefer to use radiation dose (measured in rem), rather than concentrations. MDIFF has the option of estimating dose by multiplying the calculated TIC by a dose conversion factor. This method treats dose as being directly proportional to TIC. However, this assumption is not completely accurate since nonlinear factors such as decay and deposition affect dose values. However, in many cases, the direct conversion is reasonably accurate and provides a good estimate for emergency response operations.

The dose conversion factors are calculated from the output of an RSAC5 simulation. RSAC5 is a computer dose model approved for use in the INEEL Emergency Operation Center. It uses a straight line Gaussian transport model to calculate material transported by the wind and performs a complete dose calculation. The dose conversion factors are calculated as follows:

$$\mathbf{f} = \frac{\mathbf{d}}{\mathbf{TIC}} \quad (11)$$

where f is the dose conversion factor, d is the radiological dose calculated by RSAC5, and TIC is the total integrated concentration calculated by the straight line Gaussian model used in RSAC5 assuming a unit release (i.e. total amount of material released = 1). Multiplying the TIC calculated by MDIFF by f then generates an estimated dose which accounts for wind variations that can not be included in the RSAC5 straight line Gaussian model.

A dose conversion factor may be calculated for any point in the area of impact. If deposition or decay is a significant factor, the dose conversion factor will vary with the time the material has been in transit. By making this calculation at different downwind distances, the dose conversion factor may be calculated as a function of travel time.

The dose conversion factors calculated in this manner are specific for the release inventory used in the RSAC5 simulation. Consequently, a different set of ratios must be calculated for different release inventories. Scenarios have been developed for many potential events that might occur at facilities at the INEEL. For these scenarios, dose conversion factors have been pre-calculated using RSAC5. These scenarios can be simulated by simply selecting the desired scenario at run time. For releases that can not be approximated by one of these pre-determined scenarios, RSAC5 must be simulated off-line to generate a file of dose conversion factors based on the best estimates of the release inventory. The MDIFF user then would specify this newly created file to simulate the event.

This page intentionally left blank.

MDIFF Evaluation

Tracer experiments for the purpose of atmospheric transport and diffusion model evaluations are expensive and difficult to conduct. Fortunately, data that could be used for a partial evaluation of the MDIFF model were available as part of an atmospheric tracer experiment conducted in 1999 (Clawson et al., 2000). For this experiment, a 21 m release stack was set up near the Grid III location on the INEEL. Three sampling arcs ranging in distance from 15 to 50 km northeast of the release site were established along existing roads and trails. One additional arc was placed about 20 km south of the release site. Fixed sampling positions were established on these arcs for purposes related to the overall experimental objectives. These arcs were designated A, B, C and D. Their locations, together with the fixed sampling positions, are shown in Fig. 6. The goal for the test series was to sample an intentionally released atmospheric tracer at distances of 15 to 50 km downwind. Therefore, the tests were usually conducted under conditions of strong and rather steady winds. Six 4-hour and one 2-hour tracer releases from the release stack were conducted in April and May of 1999.

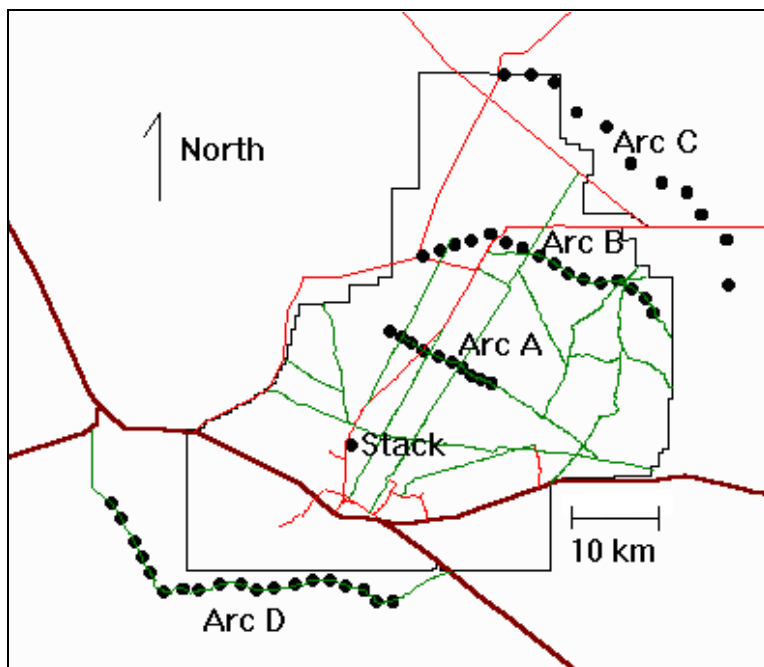


Figure 6. Location of the tracer release stack and tracer sampling arcs.

A summary of the release and sampling dates and times are given in Table 3. The tracer sulfur hexafluoride (SF_6) was released from the release stack during the tests. Two mobile real-time SF_6 detection instruments were placed in vans and deployed during each test, usually on each of two sampling arcs. During each test, the vans traversed the arcs measuring SF_6 along the way.

The MDIFF model was used in real-time to calculate plume location and concentration during each release. This information was used to direct the sampling vans to intersect the plume during and immediately following a release. During the tests, casual comparisons of calculated plume locations and concentrations with real-time actual measurements of SF_6 indicated good agreement. Subsequently, a more substantial model evaluation effort was undertaken to better understand model performance.

Table 3. Atmospheric tracer test summary.

Test #	Date (1999)	Start Time (MDT)	End Time (MDT)	Plume Tracking End Time (MDT)	Wind Direction (Degrees)	Wind Speed (m s ⁻¹)	Air Temp. (C)	Stability Category
1	19 Apr	1400	1600	1700	205 to 245	11 to 13	19.2 to 17.2	B to D
2	23 Apr	1300	1700	1745	036 to 052	13 to 12	10.6 to 11.6	D
3	26 Apr	1245	1645	1745	221 to 246	10 to 12	17.8 to 16.1	C to D
4	27 Apr	1300	1650	1740	223 to 150	7 to 6	13.6 to 9.6	B to D
5	02 May	1230	1623	1730	219 to 230	9 to 12	7.8 to 7.3	B to D
6	07 May	1300	1700	1800	231 to 241	12 to 12	16.8 to 16.3	C to D
7	07 May – 08 May	2215	0215	0345	216 to 257	7 to 4	8.5 to 0.8	F

Time History Comparisons

Since continuous tracer measurements were not available for analysis, the following technique was used to compare modeled and measured SF₆ concentrations. Model and SF₆ analyzer concentrations were calculated for matching five-minute periods. During each of these periods, SF₆ analyzer concentrations were assigned to the average van position for the period. It was assumed that this did not introduce serious errors since the arc roads on which the vans drove were very rough and van speed was frequently reduced to 1-2 m s⁻¹. The average SF₆ analyzer concentrations were plotted at the average van positions over each five-minute period. When the modeled plume was overlaid on these plots, one could qualitatively compare the model and measured SF₆ concentrations. Fig. 7 is an example of this type of plot. The results of these comparisons were very encouraging. Most of the time the SF₆ analyzers measured the plume in the locations the model had predicted. In order to examine the time history of both modeled and measured concentrations at a given location, receptor positions were defined along each of the arcs. When the average van position was within 1 km of a receptor position, the average SF₆ analyzer concentration was assigned to that receptor. This made it possible to compare the model and SF₆ analyzer measurements at a fixed location in time.

Figure 5 is an example of a time history plot comparing modeled and measured concentrations at one of the defined receptor positions. Due to the mobile sampling pattern of the SF₆ analyzers, a receptor location had actual SF₆ measurements only when a van was in the area. The case shown in Fig. 5 is one where the van made several passes during the time period that the model was predicting the plume to be in the area. The model calculations and SF₆ analyzer measurements in this case were in good agreement.

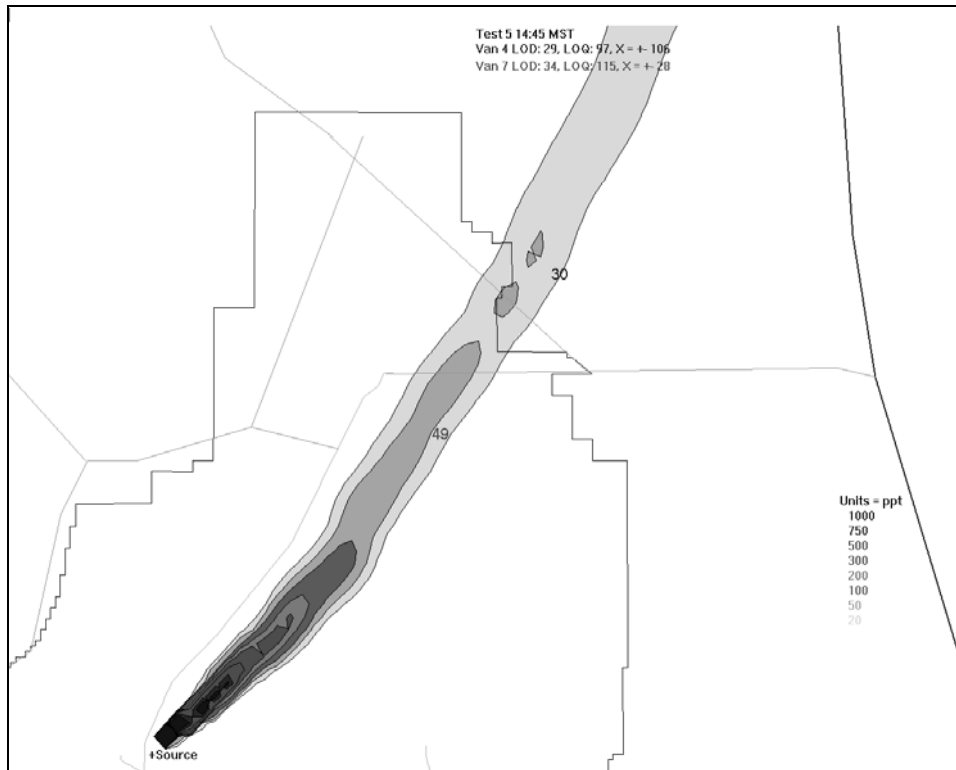


Figure 7. Example model concentration isopleth and SF₆ analyzer concentration from Test 5 at 14:45 MDT. The two numbers represent the measured SF₆ concentration at the location of the measuring equipment.

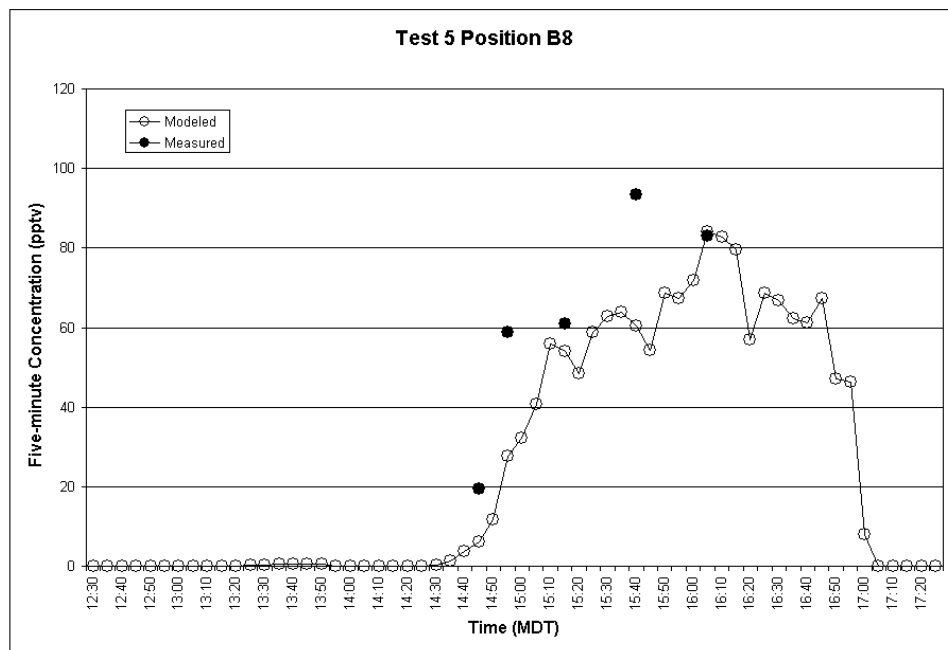


Figure 8. Time history graph of modeled and measured average 5-minute SF₆ concentrations at receptor site B8 during Test 5.

In order to examine model bias, ratios of model calculations to SF₆ analyzer measurements were constructed for all SF₆ analyzer measurements that exceeded 28 pptv. Measurements less than 28 pptv were not considered since that was the average limit of detection of the SF₆ tracer. From Table 3 it can be seen that the first six tests were conducted during the daytime under unstable or neutral atmospheric stability conditions. The last test was a nocturnal test conducted under stable conditions. For the purposes of comparison, the daytime tests were considered as one group and the nighttime test was considered separately. Averages of the model/SF₆ analyzer ratios were computed in two ways. First a bulk ratio of modeled concentrations to van measurements was made by computing the average model concentration and average van measurements over each arc and then calculating model/SF₆ analyzer ratios from these bulk averages. In the second method, model/SF₆ analyzer ratios were computed for each valid SF₆ analyzer measurement and the average of the individual ratios was determined for each arc. This calculation was called the individual ratio. Table 4 contains the results for the daytime tests.

Table 4. Comparisons of daytime modeled/measured SF₆ concentration ratios.

Arc	Location	Bulk Ratio	Individual Ratio	Number of Data Points
A	15 km north	2.9	3.6	42
D	20 km south	1.2	1.3	11
B	30 km north	0.7	0.7	31
C	50 km north	0.6	0.6	2

In the daytime tests it can be seen that the model bias varied as a function of distance. At the nearest arc, the model tended to over-predict the measured SF₆ concentrations by about a factor of three. Proceeding to the more distant arcs the model tended to over-predict slightly at Arc D and under-predict by about a factor of 1.5 at Arcs B and C. There was little difference in the two averaging methods. In general, the model did well in predicting the area of impact for the daytime tests. There were no cases where tracer was found that the model did not predict some concentration, and only four cases where the model calculations were near zero concentration. Overall, model calculations were within a factor of three 56% of the time and within a factor of five 79% of the time in daytime conditions.

The nighttime test proved to be more of a challenge for the model. Bulk and individual ratios are given in Table 5. The SF₆ was measured in areas where the model predicted it to be, but SF₆ was also measured in areas where the model predicted no impact. This was especially true for the receptor sites on Arc B where the model failed to predict a significant impact for nearly 50% the SF₆ analyzer measurements. In three cases, the model calculated no concentration and in twelve cases it predicted only plume edge effects. Apparently the plume split in the stratified nighttime air and the model only predicted a portion of the total plume trajectory. In the nighttime test, the model calculations were within a factor of three about 45% of the time and within a factor of five 52% of the time. When the model prediction was within a factor of five of

the measured concentration, it was also usually within a factor of three of the measured concentration. This implies that the model either predicted the plume concentration fairly well or it missed it entirely. The fact that the model failed to determine the whole footprint of the plume probably accounts for the marked difference in the results of the two methods of calculating model/measured ratios.

Table 5. Comparisons of nighttime modeled/measured SF₆ concentration ratios.

Arc	Location	Bulk Ratio	Individual Ratio	Number of Data Points
A	15 km north	0.4	1.9	40
D	20 km south	1.0	1.8	31

This page intentionally left blank.

Future Improvements

The use of stability classes to calculate the diffusive power of the atmosphere has been widely used in diffusion modeling. While it is useful as a working approximation of the atmosphere, it is not physically accurate. Future work with MDIFF might consider determining diffusion through the use of stability categorizations based on indexes of Richardson number or Monin-Obukhov length. The power law wind profile that MDIFF uses to adjust wind speeds for height is also based on the somewhat artificial system of stability classes. A more physically appealing approach to this calculation might be the Businger-Dyer method (Businger, et al., 1971).

Yet another improvement that could be made to MDIFF is the inclusion of a wind-field model that includes some physical properties. MDIFF currently uses only a mathematical calculation to determine the wind-field based on the inverse square of the distance to a mesonet station. A mass consistent model would inherently include a terrain-following capability that would prevent flow over mountains under stable conditions and provide for flow over mountains during unstable conditions. Furthermore, forecast wind-fields could be built on prognostic mesoscale models that exhibit terrain-forced winds.

This page intentionally left blank.

References

- Bowen, B. M., J. M. Dewart, and A. I. Chen, 1983. Stability class determination: A comparison for one site. Proceedings of the Sixth Symposium on Turbulence and Diffusion, American Meteorological Society, Boston, MA, 211-214.
- Briggs, G. A., 1969. Plume rise, USAEC Critical Review Series, TID-25075.
- Briggs, G. A., 1973. Diffusion estimation for small emissions, ATDL Contribution File No. 79, Atmospheric Turbulence and Diffusion Laboratory, NOAA, Oak Ridge, TN.
- Businger, J. A., J. C. Wyngaard, Y. Izumi, and E. F. Bradley. 1971. Flux-profile relationships in the atmospheric surface layer. J. Atmos. Sci. 28:181-189.
- Clawson, K. L., J. F. Sagendorf, R. G. Carter, 2000. Comparisons of a puff trajectory model with real-time measurements, Proceedings of the 11th Joint Conference on the Applications of Air Pollution Meteorology with Air and Waste Management Association, American Meteorological Society, 9-14 January 2000, Long Beach, California, 293- 298.
- Clawson, K. L., G. E. Start, N. R. Ricks 1989. Climatology of the Idaho National Engineering Laboratory 2nd Edition, DOE/ID-12118, U. S. Dept. of Energy Idaho Operations Office, 155 pp.
- U.S. EPA, 1993. On-Site meteorological program guidance for regulatory modeling applications (Revised). EPA-600/3-88-043. Office of Air Quality Planning and Standards, U.S. Environmental Protection Agency, Research Triangle Park, NC, 171 pp.
- Fuquay, J. J., C. L. Simpson, and W. T. Hinds, 1963. Prediction of environmental exposures from sources near the ground, based on Hanford experimental data. Hanford Atomic Products Operation, General Electric Co., Richland, WA.
- Gifford, F. A., 1976. "Turbulent diffusion typing schemes – a review", Nuclear Safety 17:68-86.
- Markee, E. H., Jr., 1963. Methods of estimating air pollutant dispersion over relatively smooth terrain from routine meteorological observations. Tech. Rep. Presentation. At the 219th Nat. Mtg. Of the American. Meteorological. Soc., 20 June 1963, at Palo Alto, CA. U.S. Dept. of Commerce, U. S. Weather Bureau., Idaho Falls, ID.
- Slade, D. H. (ed.), 1968. Meteorology and Atomic Energy 1968, TID-24190, ESSA, Air Resources Laboratories, Silver Spring, Md. 445 pp.
- Start, G. E. and L. L. Wendell, 1974. Regional effluent dispersion calculations considering spatial and temporal meteorological variations, NOAA Tech. Memo, ERL ARL-44, 63 pp.

Ramsdell, J. V., G. F. Athey, C. S. Glanz, 1983. MESOI Version 2.0: An interactive mesoscale lagrangian puff dispersion model with deposition and decay, NUREG/CR-3344 PNL-4753, 195 pp.